Neo-sex chromosome evolution shapes sex-dependent asymmetrical introgression barrier

Silu Wang[a], Matthew J. Nalley[a], Kamalakar Chatla[a], Reema Aldaimalani[a], Ailene MacPherson[b], Kevin H.-C. Wei[a], Russell B. Corbett-Detig[c], Dat Mai[a], and Doris Bachtrog[a,1]

Sex chromosomes play a special role in the evolution of reproductive barriers between species. Here we describe conflicting roles of nascent sex chromosomes on patterns of introgression in an experimental hybrid swarm. *Drosophila nasuta* and *Drosophila albomicans* are recently diverged, fully fertile sister species that have different sex chromosome systems. The fusion between an autosome (Muller CD) with the ancestral X and Y gave rise to neo-sex chromosomes in *D. albomicans*, while Muller CD remains unfused in *D. nasuta*. We found that a large block containing overlapping inversions on the neo-sex chromosome stood out as the strongest barrier to introgression. Intriguingly, the neo-sex chromosome introgression barrier is asymmetrical and sex-dependent. Female hybrids showed significant *D. albomicans*–biased introgression on Muller CD (neo-X excess), while males showed heterosis with excessive (neo-X, *D. nasuta* Muller CD) genotypes. We used a population genetic model to dissect the interplay of sex chromosome drive, heterospecific pairing incompatibility between the neo-sex chromosomes and unfused Muller CD, neo-Y disadvantage, and neo-X advantage in generating the observed sex chromosome genotypes in females and males. We show that moderate neo-Y disadvantage and *D. albomicans* specific meiotic drive are required to observe female-specific *D. albomicans*–biased introgression in this system, together with pairing incompatibility and neo-X advantage. In conclusion, this hybrid swarm between a young species pair sheds light onto the multifaceted roles of neo-sex chromosomes in a sex-dependent asymmetrical introgression barrier at a species boundary.

hybridization | neo-sex chromosome | Y degeneration | inversion | meiotic drive

Speciation is a fundamental process that generates the diversity of life (1), yet the underlying genomic mechanisms of speciation are not well understood (2–5). There has been accruing evidence of sex chromosomes disproportionately accumulating genomic differentiation among diverging lineages (6–9), termed the "large X/Z effect" (10). However, the interaction of sex chromosome evolution and genomic differentiation underlying early speciation remains an open question (11). That is, what is the effect of sex chromosome evolution and differentiation on the extent and direction of introgression across species boundaries? An ideal system to investigate this question would encompass lineages in the early stage of speciation, in which newly formed sex chromosomes, such as neo-sex chromosomes, evolve as speciation unfolds (12, 13). In such systems where reproductive isolation is still incomplete, the direction and extent of introgression on autosomes, the ancestral sex chromosomes, and the neo-sex chromosomes can allow us to uncover the roles of meiotic drive and neo-sex chromosome differentiation and degeneration in the evolution of nascent species boundaries.

The sister species *Drosophila albomicans* (distributed from Japan and China to northeast India) and *Drosophila nasuta* (found in East Africa, Sri Lanka, and the India subcontinent) diverged around 0.15 to 0.5 Mya (14, 15). These species are indistinguishable morphologically and show little to no premating isolation (16, 17) and only weak hybrid breakdown in advanced generation hybrids (18, 19) but have distinct sex chromosome configurations. *D. nasuta* harbors the ancestral karyotype of this species group (2n = 8), while *D. albomicans* has a neo-sex chromosome pair, formed by the fusion of an autosome (Muller CD) and the ancestral sex chromosomes (Muller A) around 0.12 Mya (20–22) (Fig. 1A). Genetic studies have suggested that the neo-sex chromosomes evolved sequentially, with the X/Muller-CD fusion (the neo-X) being selectively favored over the ancestral unfused chromosomes and subsequently driving the fixation of the Y/Muller-CD fusion (the neo-Y chromosome) to overcome meiotic structural incompatibilities (23). Thus, this species pair provides a unique opportunity to investigate the role of sex chromosome evolution in speciation.

Significance

It is increasingly recognized that sex chromosomes are not only the battlegrounds between sexes but also the Great Walls fencing off introgression between diverging lineages. Here we dissect the multifaceted roles of sex chromosomes using experimental evolution, whole-genome resequencing, and theoretical modeling, taking advantage of hybrid populations between a *Drosophila* sister species pair in the early stage of speciation that have different sex chromosome systems. Our work sheds light onto the complex roles of neo-sex chromosome evolution in creating a sex-dependent asymmetrical introgression barrier at a species boundary, and we show how diverse population genetic forces act in concert to explain observed patterns of introgression across the genome.
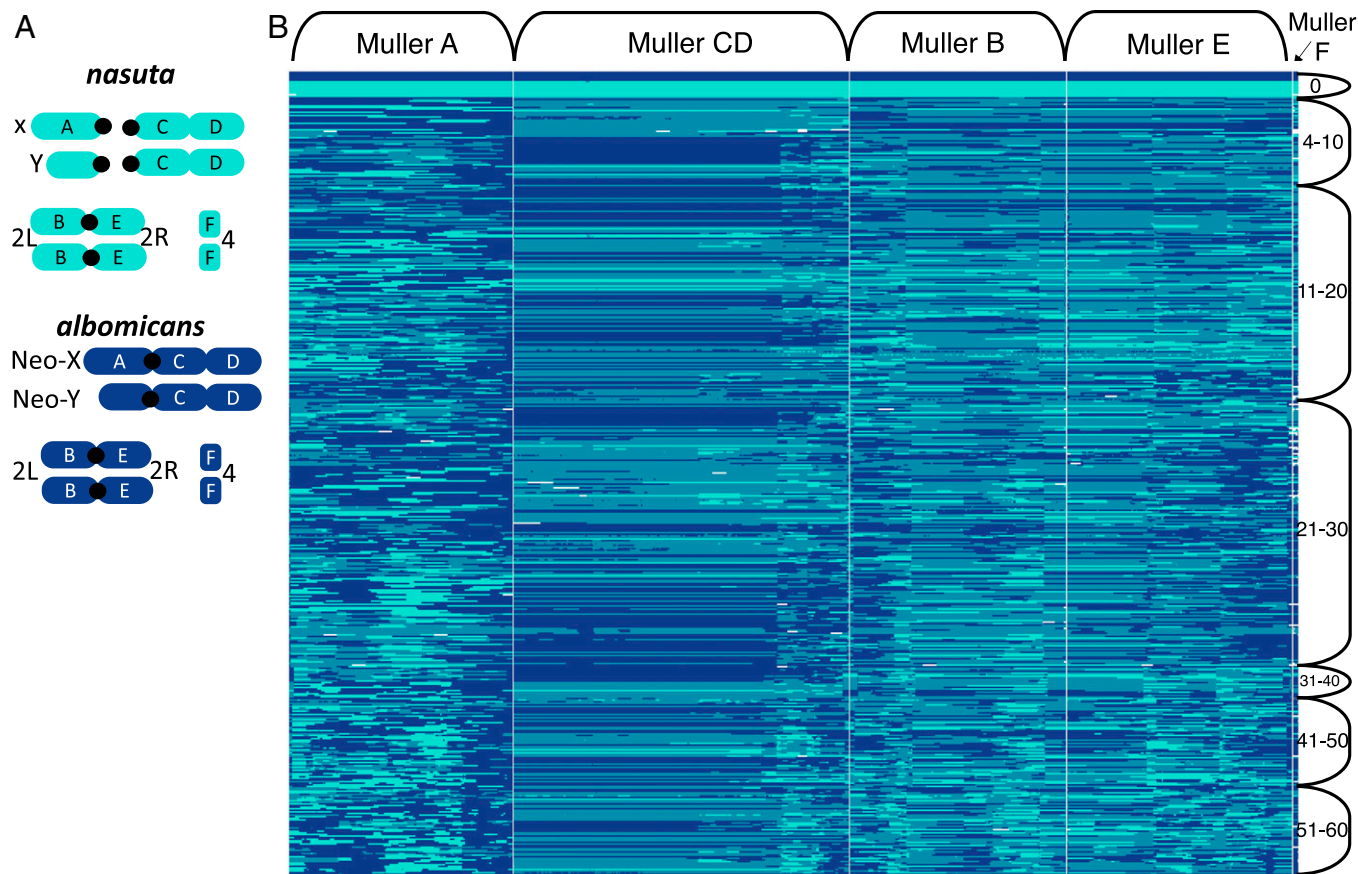
Fig. 1. Genotypes and admixture between *D. albomicans* and *D. nasuta* ancestry. (*A*) Karyotype of *D. albomicans* and *D. nasuta*. Muller CD and Muller A are separate chromosomes in *D. nasuta* but fused in *D. albomicans*, forming a neo-X or neo-Y chromosome. (*B*) Ancestry HMM of haplotypes (in columns) in hybrids sampled from a range of generations (rows, numbered on the right). The turquoise and royal blue represent homozygous *D. nasuta* and *D. albomicans* genotypes, respectively, and the heterozygous genotypes are represented by pale blue.

Neo-sex chromosomes may play a role in the formation of new species. In Japanese threespine stickleback fish, a sex chromosome–autosome fusion brought together loci responsible for behavioral isolation and hybrid sterility (12). Neo-sex chromosomes are also common in Lepidoptera, and it was suggested that they contribute to ecological specialization and species formation (24). Genomic patterns of population differentiation and admixture also supported an important role for newly formed neo-sex chromosomes in evolving reproductive isolation in mountain pine beetle populations (13).

Here we investigated the role of the neo-sex chromosomes on patterns of genomic differentiation over more than 62 generations of hybridizations between *D. albomicans* and *D. nasuta*. Hybrid swarms undergoing hybridization over multiple generations can reveal the extent and direction of introgression in different parts of the genome and allow us to investigate the role of sex chromosomes contributing to genomic differentiation. Specifically, tracking ancestry turnover in the neo-sex chromosome relative to the rest of the genome can reveal the role of sex chromosome evolution in shaping patterns of introgression.

The evolution of neo-sex chromosomes could shape introgression between *D. nasuta* and *D. albomicans* multiple ways. The fused neo-X could be selectively favored over the unfused *D. nasuta* karyotype, as suggested by hybrid crosses (25); this could facilitate the spread of the neo-X in the hybrid population. Increased pairing compatibility of the neo-X and neo-Y during male meiosis could indirectly facilitate neo-Y introgression at high frequency of the neo-X (23). On the other hand, the neo-X could also limit or promote the spread of the neo-Y

due to meiotic drive. Notably, a polymorphic sex ratio drive was discovered in crosses between *D. albomicans* strains from Japan and *D. nasuta* strains from India (26) and in interspecific crosses between *D. albomicans* and *D. nasuta* (27). Thus, the neo-X may harbor meiotic drive alleles that are toxic to neo-Y carriers in certain *D. albomicans* strains (26, 27), and (some) neo-Y chromosomes may harbor suppressors for drive that are absent in *D. nasuta*, which would limit or promote the spread of the neo-Y, respectively. In addition, accumulation of frameshift mutations and lower gene expression was observed for a subset of neo-Y genes (21). Beginning degeneration of the neo-Y incurs a fitness disadvantage over the unfused *D. nasuta* homologous Muller-CD chromosomes and could select against the neo-Y chromosome in male hybrids. Altogether, the *D. nasuta*/*D. albomicans* system provides an opportunity to uncover and dissect the multifaceted roles of neo-sex chromosome evolution in introgression.

Although this species pair is predominantly allopatric and typically does not form secondary contact in nature, artificial hybrid populations provide a valuable opportunity to investigate the effect of neo-sex chromosome evolution on patterns of introgression between these otherwise similar lineages. Here we generated replicate hybrid swarms of *D. nasuta* and *D. albomicans* and sequenced almost 450 sampled hybrid individuals over 62 generations. In particular, we ask 1) what is the extent and direction of introgression at the species boundary, 2) does the direction and extent of introgression within neo-sex chromosomes differ from the rest of the genome, and 3) do sexes differ in introgression? We address these questions accounting

for chromosomal inversions, neo-X advantage, neo-Y degeneration disadvantage, neo-X meiotic drive, and heterospecific pairing incompatibility. Furthermore, we use a population genetic model to formulate a comprehensive understanding of the role of the multiple interacting evolutionary processes shaping introgression in this system. Specifically, we ask 4) under which combinations of neo-X meiotic drive, neo-X advantage, neo-Y degeneration disadvantage, and heterospecific chromosomal pairing incompatibility do we expect to observe the sex-specific genotypic frequency of Muller CD as we did in the experiment?

Methods

Hybrid Swarm and Sampling. We used *D. nasuta* strain 15112-1781.00 (from Mysore, India) and *D. albomicans* strain 15112-1751.03 (from Nankang, Taiwan) to construct admixed populations (hybrid swarms). These strains have chromosome-level genome assemblies and differ by two fixed inversions on Muller-CD (28). We set up reciprocal interspecific crosses (i.e., we crossed 30 *D. nasuta* virgin females with 30 *D. albomicans* males and 30 *D. albomicans* virgin females with 30 *D. nasuta* males) and mixed all of the resulting F_1 offspring to initiate the hybrid swarm. The hybrid swarm was maintained in large Plexiglass population cages (dimensions being $12'' \times 12'' \times 12''$). The population cages were kept at humidity 48% and a 12-h light–dark cycle with lights on during 8 AM to 8 PM. Each week, we added two new molasses bottles of fly food (standard corn medium); these bottles were removed from the cages 4 wk later, all adults in the bottles were discarded, and newly emerging flies from the sample bottles were collected and frozen about 1 wk later. To assess repeatability of the introgression outcome, we set up two independent replicates of the hybrid swarm (one in 2014 and one in 2018) following the crossing scheme described above. In addition, we also set up another population cage in 2014 where we directly combined 30 adults of each sex from both species to initiate a hybrid swarm (*SI Appendix*, Fig. S6); this cage was maintained as described above but only sampled at generations 27 and 28. Generations of sampled flies were determined based on sampling date, assuming a generation time of 14 d.

DNA Isolation, Library Preparation, and Sequencing. We sequenced a total of 232 females and 215 males sampled from select generations (between 3 and 62; *SI Appendix*, Table S1). The detailed sample size in terms of sex and generation is summarized in *SI Appendix*, Table S1. DNA extractions were performed as described in ref. 26 with modifications as follows. Flies were crushed in Puregene lysis buffer (120 μL) using the Mixer Mill 400 at 30 Hz for 3 min. Lysate (100 μL) was treated with RNase A, and protein was precipitated with Puregene protein precipitation solution (33 μL) on ice for 30 min. Clarified lysate (80 μL) was transferred to ice cold isopropanol (80 μL), mixed well, and incubated for 30 min. DNA was precipitated at maximum speed for 30 min. Pellets were washed with 70% ethanol (120 μL), air dried for 15 min in a fume hood, and resuspended in Qiagen EB (20 μL). DNA libraries were prepared using the Illumina Nextera DNA library Prep kit (29) with modifications as follows. DNA was tagmented at 55°C for 5 min. The adapter PCR program is 72°C for 3 min; 98°C for 2 min 45 s; eight cycles of 98°C for 15 s, 62°C for 30 s, and 72°C for 90 s; and hold at 4°C. An additional four cycles of reconditioning PCR were also performed. Libraries were pooled and size selected using AmpureXP to remove fragments <200 bp and minimize fragments >800 bp. Sequencing was performed on a Hiseq 4000 with 100 bp paired-end reads.

Sequence Processing. Code involved in the pipeline has been deposited in GitHub (https://github.com/setophaga/hybridswarm.alb.nas). Briefly, we trimmed the reads with trimmomatic (29), with the following specification: -phred33 TRAILING:3 SLIDINGWINDOW:4:10 MINLEN:30. For some libraries, flies from up to four different species group were combined prior to DNA extraction, and reads were separated bioinformatically. In particular, we aligned the trimmed reads to the concatenated genome including the closest outgroup *Drosophila kepuluana* genomic reference (30), as well as *Drosophila pseudoobscura* (GenBank: PRJNA596268), *Drosophila virilis* (GenBank: PRJNA475270), and *Drosophila athabasca* (31), with bwa (32). Individuals with fewer than 50,000 mapped reads were excluded from downstream analysis.

Reference Haplotypes. To construct a parental ancestry haplotype reference, we used the existing high-coverage sequencing data of alb03 line (two males, DBMN30-16_S49_L008 and DBMN30-19_S51_L008, and one female, DBMN21-D_S4_L007) and nas00 line (DBCC035C4_S68_L008 and DBMN21-B_S2_L007) (30). We aligned the reads to the same *D. kepuluana* reference (see *Sequence Processing*) before genotyping with GATK 3.8. To determine *D. albomicans* vs. *D. nasuta* specific alleles, we calculated allele frequency within each species with VCFtools (33) and selected the sites with allele frequency difference greater than 0.3. Within *D. albomicans*–specific alleles, we determined whether a Muller CD alleles is neo-Y or neo-X specific following our previous study (21). Briefly, we regarded neo-sex chromosome-specific sites as those within Muller CD that are homozygous in females and heterozygous in males.

Ancestry Calling. Ancestry HMM (34) was used to infer local genomic ancestry among hybrids in the hybrid swarm experiment. The following setting was employed: -a 2 0.5 0.5 -p 0-3 0.5 -p 1-3 0.5 -r 0.000005. In particular, we assumed equal parental ancestry contributions and recombination rate being 5×10^{-6} and estimated the generations before present in which the ancestry pulse occurred. We first found the ancestry informative single-nucleotide polymorphisms with allele frequency difference >0.3 between the *D. nasuta* strain and *D. albomicans* strain. Then we prepared the input for ancestry HMM with a custom script. We defined 0 = *D. nasuta*, 0.5 = heterozygotes, and 1 = *D. albomicans*. Ancestry genotype was only called if the maximum posterior probability > 0.9, when the maximum posterior probability genotype was assigned to the locus.

Neo-Sex Chromosome Haplotyping. Within Muller CD, we needed to delineate neo-X, neo-Y, versus *D. nasuta* ancestry blocks. To do so, we ran a secondary three ancestry types analysis within ancestry HMM for sites within Muller CD, -a 3 0.3325 0.3325 0.335 -p 0-3 0.3325 -p 1-3 0.3325 -p 2-3 0.335 -r 0.000005. A Muller CD haplotype was called if the maximum posterior probability > 0.9. For each individual, we estimated the haplotype proportion (proportion of sites of each haplotype across all the haplotype-informative sites). With this information, we could track the haplotype and genotype frequency over time. Codes in the pipeline are deposited in GitHub (https://github.com/setophaga/hybridswarm.alb.nas).

Genomic Barriers to Introgression. We identified genomic barriers to introgression based on reduced ancestry junctions as well as the lack of admixture inferred from heterozygosity–ancestry relationships. Genomic barriers to introgression are expected to harbor reduced ancestry turnovers and suppression of admixture. We estimated ancestry turnover rate by the number of ancestry turnovers over the total ancestry informative sites in each Muller element. To test if there is difference in ancestry turnover rates, we employed Pearson's χ^2 test with input being a contingency table of counts of ancestry junctions over total ancestry informative sites in each Muller element.

In addition, we considered genomic local admixture as a function of ancestry score (with 0 and 1 being pure *D. nasuta* and *D. albomicans*, respectively) and interspecific heterozygosity. Heterozygosity is expected to decay as admixture progresses. To control for pseudoreplication due to linkage among ancestry informative sites, we first identified genetic clusters within which the ancestry blocks tend to cosegregate among all the hybrids (35). Specifically, with R function *kmeans*, we iteratively incremented k (from k = 1) until 60% of the total variance was explained by between-clusters variance. For each K-means cluster, we calculated the barrier effect (the γ index) as a function of heterozygosity (h), the fraction of heterozygous ancestry-informative sites within each individual, and admixture proportion (p), the fraction of *D. albomicans* alleles across ancestry-informative sites.

$$\gamma = \sqrt{(2(p - 0.5))^2 + h^2}.$$

This index effectively represents the adjusted distance between the coordinate of each hybrid and the admixture maxima, where $P = 0.5$ and $h = 0$, in the triangle space delineated by ancestry on the x axis and heterozygosity on the y axis. The γ variable effectively reflects the position of each hybrid in the triangle plot, which is widely used to infer hybrid identity (36). The mean γ of a set of hybrids sampled at a time point reflects the extent of admixture within a genomic region of interest. The greater the barrier effect, the less admixture occurs within the

genetic cluster, and the greater distance the hybrids are from the point of admixture maxima. To compare the barrier effect γ among different Muller elements, we employed ANOVA followed by post hoc paired-t test with Bonferroni correction. Because the ancestral Y is largely pseudogenized and degraded, γ is not applicable for Muller A in males.

Muller CD Introgression. To compare patterns of introgression in Muller CD versus the rest of the genome, we examined the ancestry proportion, interspecific heterozygosity, linkage disequilibrium (LD), and genomic clines (37) of Muller CD relative to the rest of the genome.

For each K-means cluster (*Genomic Barriers to Introgression*), we fit the Muller CD genomic cline (37) in which the mean ancestry of Muller CD clusters is the mean ancestry of all the K-means clusters genome-wide. In the course of admixture, local ancestry relative to genome-wide ancestry reflects the extent and direction of introgression of a genomic region. The genomic cline function $\theta = p + (2\,(p - p^2) \times (\alpha + (\beta\,(2p) - 1))$, where θ is the local ancestry of Muller CD and p is the genome-wide ancestry; α and β represents the direction and extent of the barriers' effect of the genomic region, respectively. If Muller CD introgressed similarly as the rest of the genome, α and β should be zero. A significant barrier effect of Muller CD would be reflected by a positive β. If there is disproportionally *D. albomicans*–biased introgression within Muller CD, α should be significantly positive, whereas *D. nasuta*–biased introgression corresponds to a negative α value. Under the neo-X advantage hypothesis, we expect a significantly positive α in hybrids.

Another representation of a barrier to introgression is LD. LD is expected to decay as admixture continues, while genomic barriers to introgression would preserve high LD. If Muller CD serves as a genetic barrier to introgression, LD among K-means clusters within Muller CD would remain high relative to the rest of the genome. We tested whether the mean LD is different among Muller elements. Other genomic regions that harbor epistasis with genes in Muller CD would remain in high LD with Muller CD as well.

Time Series of Haplotype and Genotype Frequencies. To understand the evolution and effect of the neo-sex chromosome, we tracked the dynamics of Muller CD ancestry (i.e., *D. nasuta* or *D. albomicans* neo-X or neo-Y) in a sex-specific manner over generations of hybridization. We modeled haplotype frequencies as time series and tested whether the time series of neo-X, neo-Y, or *D. nasuta* Muller CD haplotype frequency demonstrate autocorrelation against the null stationary model. We employed the rank von Neumann ratio test (38), with the *serialCorrelationTest* function in R. If no temporal autocorrelation was observed, we tested the deviation of the haplotype frequencies from the corresponding expected values based on 50:50 admixture. For females, the expected haplotype frequency of neo-X versus *D. nasuta* should be 0.5, while for males, the expected frequency of neo-X, neo-Y, and *D. nasuta* should be 0.25, 0.25, and 0.5, respectively. We have only included generations in which there were more than five females and five males.

In addition, we tested the pairing compatibility hypothesis in which the presence of the neo-X could facilitate an increase of neo-Y frequency due to problems in meiosis with the unfused *D. nasuta* Muller CD. If so, the neo-X frequency in females should be positively correlated with the neo-Y frequency in males, after controlling for temporal autocorrelation as the cofounding factor. We therefore used a partial Mantel test with mantel.partial function in R. Finally, we tested whether Muller CD segregation deviates from Hardy–Weinberg equilibrium by contrasting the expected genotype frequencies under random paring of haplotypes versus observed genotype frequencies with a Pearson's χ^2 test.

Population Genetic Model of Neo-Sex Chromosome Evolution. To better understand the dynamical feedback among the multiple evolutionary forces at play within the hybrid cages, we modeled the evolution of neo-sex karyotype frequencies through time as a single-locus continuous time model with separate sexes. Parental individuals were assumed to mate at random. Specifically, we ask the following: starting from the initial condition of the experiment, under which combinations of 1) heterospecific sex chromosome incompatibility, 2) conspecific and heterospecific neo-X meiotic drive, 3) neo-X selective advantage, and 4) neo-Y degeneration disadvantage would we observe the same sex-specific genotypic frequencies within Muller CD as we observed in the hybrid swarm experiment?

Here we denote *D. nasuta* X and Y chromosome and the unfused Muller CD as N_x and N_y and the X and Y of *D. albomicans* as A_x and A_y. Due to genetic incompatibilities, hybrid zygotes (N_xA_x, N_xA_y, and A_xN_y) were subject to a reduction in absolute fitness of $(1 - \rho)$. As a result of coevolution of meiotic drivers between the neo-X and suppressors on the neo-Y (but not the ancestral Y or unfused Muller CD), a meiotic driver on the neo-X chromosome results in killing of *D. nasuta* Y/Muller-CD sperm of heterozygous (neo-X, *D. nasuta* Y) with a probability of μ_H. We also include two putative within-species meiotic drivers on the neo-X and *D. nasuta* X that kill the neo-Y and the *D. nasuta* Y sperm with probability of μ_A and μ_N, respectively. Finally, we introduce a putative additive selected advantage to the neo-X of magnitude s_x and an additive disadvantage of the neo-Y of size s_y. The result is a system of seven coupled differential equations giving the frequency, F, of each karyotype. The derivation and expression of the differential equations can be found in the *SI Appendix, Supplementary Mathematica* notebook. We analyze the karyotype frequency dynamics by first identifying the biologically valid equilibria of the dynamical system. We then analytically determine the local stability of these equilibria and finally use a numerical approach to determine the global stability of the equilibria given the initial conditions of the hybrid swarm.

Fly Crosses to Estimate Sex Ratio Meiotic Drive. Five virgin *D. albomicans* females were crossed to 7 to 10 *D. nasuta* males. F_1 hybrid virgin females were backcrossed to either *D. albomicans* or *D. nasuta* males, and F_1 hybrid males were backcrossed to either *D. albomicans* or *D. nasuta* virgin females. For each of these four backcrosses, three vials of 5 virgin females by 7 to 10 males were set up, and flies were transferred to new vials every 2 to 3 d for 2 wk. Once the adult offspring started emerging, offspring were sexed and counted every day for up to 10 days. Offspring counts from different vials and transfers of the same cross were then summed.

We estimate *D. albomicans*–specific (μ_A), *D. nasuta*–specific (μ_N), and heterospecific (μ_H) meiotic drive with female and male counts with the following formula: (female counts – male counts)/female counts, as the fraction of Y gametes that were killed. We estimated *D. albomicans* and *D. nasuta*–specific meiotic drive μ_A and μ_N from backcrossing F_1 females (neo-X, *D. nasuta* Muller CD) with *D. albomicans* males (neo-X, neo-Y) or *D. nasuta* males (*D. nasuta* Muller CD, *D. nasuta* Muller CD), respectively. To estimate μ_H, we backcrossed F_1 males (neo-X, *D. nasuta* Muller CD) with *D. albomicans* females (neo-X, neo-X) or *D. nasuta* females (*D. nasuta* Muller CD, *D. nasuta* Muller CD) and took the mean of the two backcrosses.

Results

Reduced Introgression in Muller CD. Fig. 1*B* shows the inferred haplotypes of hybrids sampled over 62 generations of hybridization. There was extensive introgression and reshuffling of ancestral haplotypes in Muller A, B, and E, relative to Muller CD (Fig. 1*B* and *SI Appendix,* Fig. S1). Ancestry junction rates varied significantly among Muller elements ($\chi^2 = 11.56$, df = 3, $P = 0.009$), and the ancestry junction rate was reduced in Muller CD relative to other chromosomes (Figs. 1 and 2). The region of reduced ancestry turnover within Muller CD coincides with the two overlapping chromosomal inversions found in the strains used to generate the hybrid swarm (27) (Fig. 2).

K-means clustering drastically reduces the number of ancestry-informative units in each Muller element and minimizes pseudoreplication (*SI Appendix,* Table S2). Admixture proportions, which measure the fraction of *D. albomicans* alleles across each k-means cluster along each Muller element, were traced across generations in female versus male hybrids separately (Fig. 3). There was significant *D. albomicans*–biased introgression genome-wide in both females (mean = 0.65, t = 15.70, $P < 10^{-15}$) and males (mean = 0.59, t = 7.91, $P < 10^{-12}$), while there was heterogeneity across Muller elements (Fig. 3).

The barrier effect γ, which measures the reduction in admixture relative to the admixture maxima, was significantly
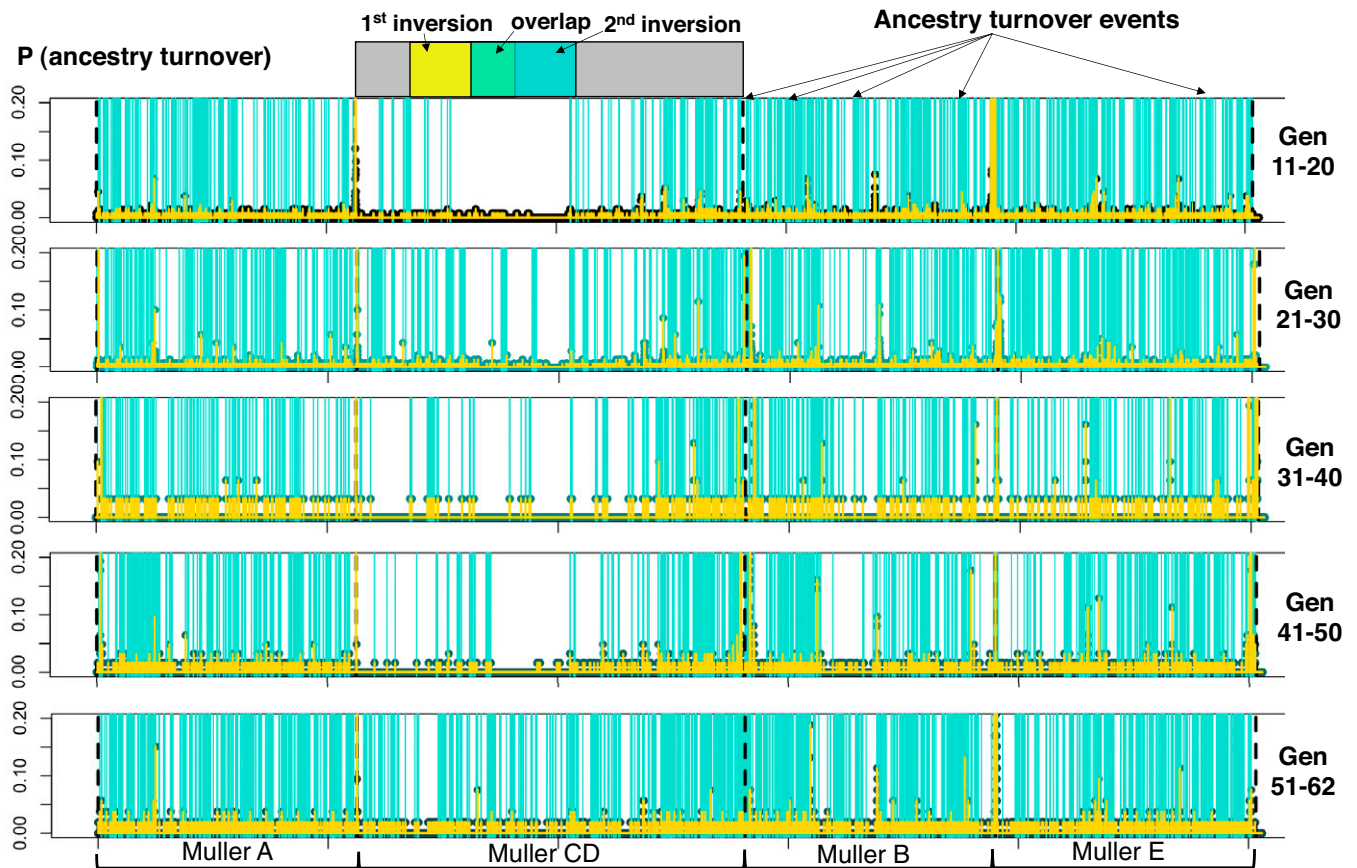
Fig. 2. Incidences of ancestry turnovers during the course of hybrid swarm evolution. Each vertical turquoise line represents an ancestry junction. The yellow peaks represent the probabilities of ancestry turnovers across chromosomal positions. The reduced ancestry turnover rate in Muller CD corresponds to two pericentromeric overlapping inversions.

elevated in Muller CD compared to other Muller elements in both sexes across all the generation intervals examined (*SI Appendix,* Fig. S2 and Table S3). The K-means clusters with the strongest barrier effect are associated with the overlapping inversion within Muller CD. Another measure of a barrier to introgression is LD. LD remained high after 62 generations of hybridization within Muller CD, while LD decays over the course of admixture in most of the genome (Fig. 4 and *SI Appendix,* Fig. S3). The mean pairwise LD was significantly longer within Muller CD than other Muller elements ($P <$ 0.05; *SI Appendix,* Fig. S3). In addition, some long-ranged LD was observed between Muller B and Muller E (Fig. 4). Consistent with elevated levels of LD, disproportionately fewer ancestry turnover events (0.83%) are detected in Muller CD, compared to Muller A (15.04%), Muller B (25.20%), and Muller E (58.92%).

Sex-Dependent Asymmetrical Introgression. Intriguingly, we find evidence for *D. albomicans*–biased introgression of Muller CD in females (admixture proportion > 0.5; Fig. 3, yellow) but not in males. The genomic cline analysis revealed significantly positive α (*D. albomicans*–biased introgression of Muller CD relative to genomic background) in generations 1 to 20 as well as 31 to 40 (Table1 and Fig. 3, yellow). In contrast, there was significantly negative α (*D. nasuta*–biased introgression) in male hybrids sampled from generations 31 to 40 (Table 1 and Fig. 3, blue). Thus, the neo-sex chromosomes/Muller CD show sex-dependent, asymmetrical introgression during the course of admixture in our experimental hybrid swarms.

Muller CD Haplotype Frequency Time Series. No significant temporal autocorrelation was observed in the Muller CD haplotype frequency for neo-X ($\rho = -0.085$), neo-Y ($\rho = -0.087$), or *D. nasuta* ($\rho = -0.096$), in females or male hybrids ($P > 0.05$), indicating the lack of directional change in haplotype frequency over the course of admixture (*SI Appendix,* Fig. S4). Different from the expectation of pairing compatibility, the residual of a linear model in which male neo-Y frequency is predicted by female neo-X frequency does not demonstrate temporal autocorrelation ($\rho = -0.47$, $P = 0.22$; *SI Appendix,* Fig. S5C). We further tested whether the mean haplotype frequencies significantly deviated from expectation. There was significantly higher neo-X frequency (mean $\pm$ SD = 0.74 $\pm$ 0.11) in female hybrids than 0.5 (effect size = 3.10, $P < 10^{-6}$), which corresponds to the significantly lower *D. nasuta* variant than expected. In contrast, the neo-Y haplotype frequency (mean $\pm$ SD = 0.12 $\pm$ 0.12) in male hybrids was significantly lower than the expected value of 0.25 (effect size = 1.55, $P = 0.0005$; *SI Appendix,* Fig. S5B). There was a higher than expected frequency of neo-X in male hybrids (effect size = 3.95, $P < 10^{-7}$), while the *D. nasuta* variant did not significantly deviate from the 0.5 expectation (effect size = 0.41, $P = 0.27$).

Neo-X advantage is evident over generations of admixture in the hybrid population (Fig. 5 *A* and *C* and *SI Appendix,* Figs. S6 and S7). While genotype frequencies fluctuate across generations and experiments, female hybrids predominantly carry (neo-X, neo-X) genotype (Fig. 5A and *SI Appendix,* Figs. S6 and S7). Across generations, the mean frequency of the (neo-X, neo-X) genotype was 0.55, which was significantly
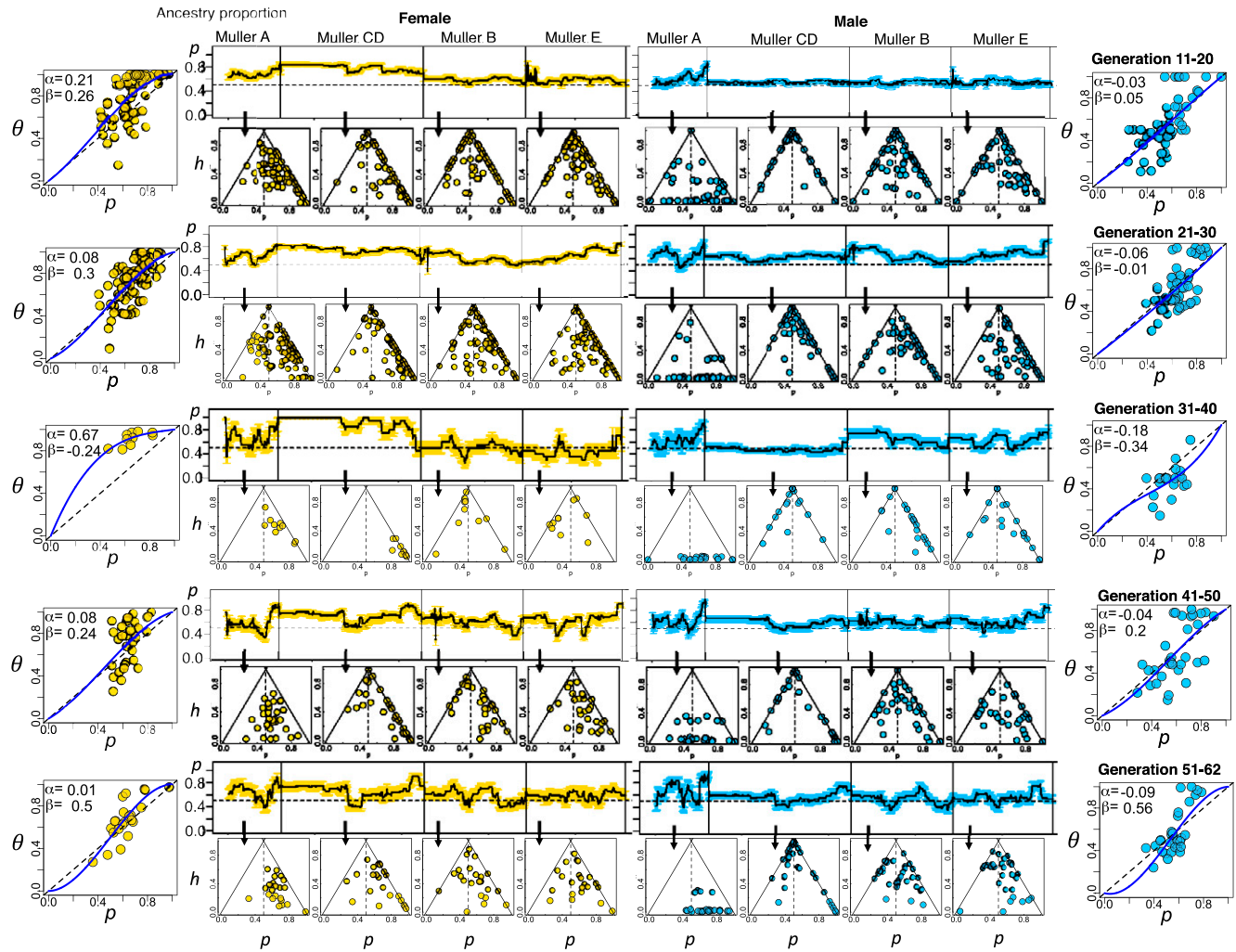
Fig. 3. Patterns of introgression along chromosomes in female versus male hybrids sampled over generations. Each row represents introgression patterns in hybrids sampled from each generation interval: 11 to 20, 21 to 30, 31 to 40, 41 to 50, and 51 to 62, with females colored in yellow and males colored in blue. The ancestry proportion scan represents the mean (± SE) admixture proportion (pure *D. nasuta*, 0; pure *D. albomicans*, 1) of each K-means cluster in Muller A, CD, B, or E in females or males sampled across generations. The triangle plots present the relationship of mean heterospecific heterozygosity (*h*) and ancestry proportion (*p*) of each Muller element. There is *D. albomicans*–biased introgression (admixture proportion > 0.5, horizontal dotted line; dots disproportionally shifted to the right arm of the triangle, alpha > 0) in Muller CD of females but not of males. The genome clines represent local ancestry (*θ*) within Muller CD relative to genome-wide ancestry (*p*) in individuals sampled from each sex at each generation. The cline parameters *α* and *β* represent the direction and extent of introgression. For *α*, positive values correspond to *D. albomicans*–biased introgression of Muller CD, whereas negative values correspond to *D. nasuta*–biased introgression. Large positive *β* corresponds to strong introgression barrier effect of Muller CD.

higher than the neutral expected frequency of 0.25 (effect size = 2.16, $P < 10^{-4}$). The mean frequency of (*D. nasuta* Muller CD, *D. nasuta* Muller CD) was 0.05, rarer than the expected mean frequency of 0.25 (effect size = 6.11, $P < 10^{-11}$). The mean frequency of heterozygous (neo-X, *D. nasuta* Muller CD) was 0.36, which is significantly lower than neutral expectation of 0.5 (effect size = 1.20, $P = 0.003$).

In contrast, we observed male-biased heterosis (Fig. 5 *B* and *D* and SI Appendix, Figs. S6 and S7), where the heterozygous genotype is more prevalent than homozygous genotypes. There was excessive heterozygous genotype of (neo-X, *D. nasuta* Muller CD) (mean frequency = 0.60) (effect size = 2.46, $P < 10^{-5}$) but deficient (*D. nasuta* X, *D. nasuta* Muller CD) (mean frequency = 0.14) (effect size = 1.44, $P = 0.001$) and (*D. nasuta* Muller CD, neo-Y) (mean frequency = 0.05) genotypes (effect size = 4.26, $P < 10^{-8}$) than their expected 0.25 neutral frequency in male hybrids (Fig. 5*D*). The (neo-X, neo-Y) frequency (mean = 0.18) did not significantly deviate from the expected value of 0.25 (effect size = 0.44, $P > 0.05$) (Fig. 5*D*).

Population Genetic Model. The system of differential equation for the karyotype frequencies exhibits three equilibria, which are stable in at least a portion of the biological parameter space. Denoting equilibrium values with a hat,

$$\hat{F}(A_x, A_x) = \frac{1 + 2s_x}{2 - s_y + s_x(3 - \mu_A) - \mu_A(1 - s_y)},$$

$$\hat{F}(A_x, A_y) = \frac{(1 + s_x - s_y)(1 - \mu_A)}{2 - s_y + s_x(3 - \mu_A) - \mu_A(1 - s_y)},$$

[1a]

$$\hat{F}(A_x, A_x) = \frac{1 + 2s_x}{2 - \mu_H(1 - \rho) + s_x(3 - \rho - \mu_H(1 - \rho)) - \rho},$$

$$\hat{F}(A_x, N_y) = \frac{(1 + s_x)(1 - \mu_H)(1 - \rho)}{2 - \mu_H(1 - \rho) - s_x(3 - \rho + -\mu_H(1 - \rho)) - \rho},$$

[1b]

$$\hat{F}(N_x, N_x) = \frac{1}{2 - \mu_N}, \quad \hat{F}(N_x, N_y) = \frac{1 - \mu_N}{2 - \mu_N}.$$
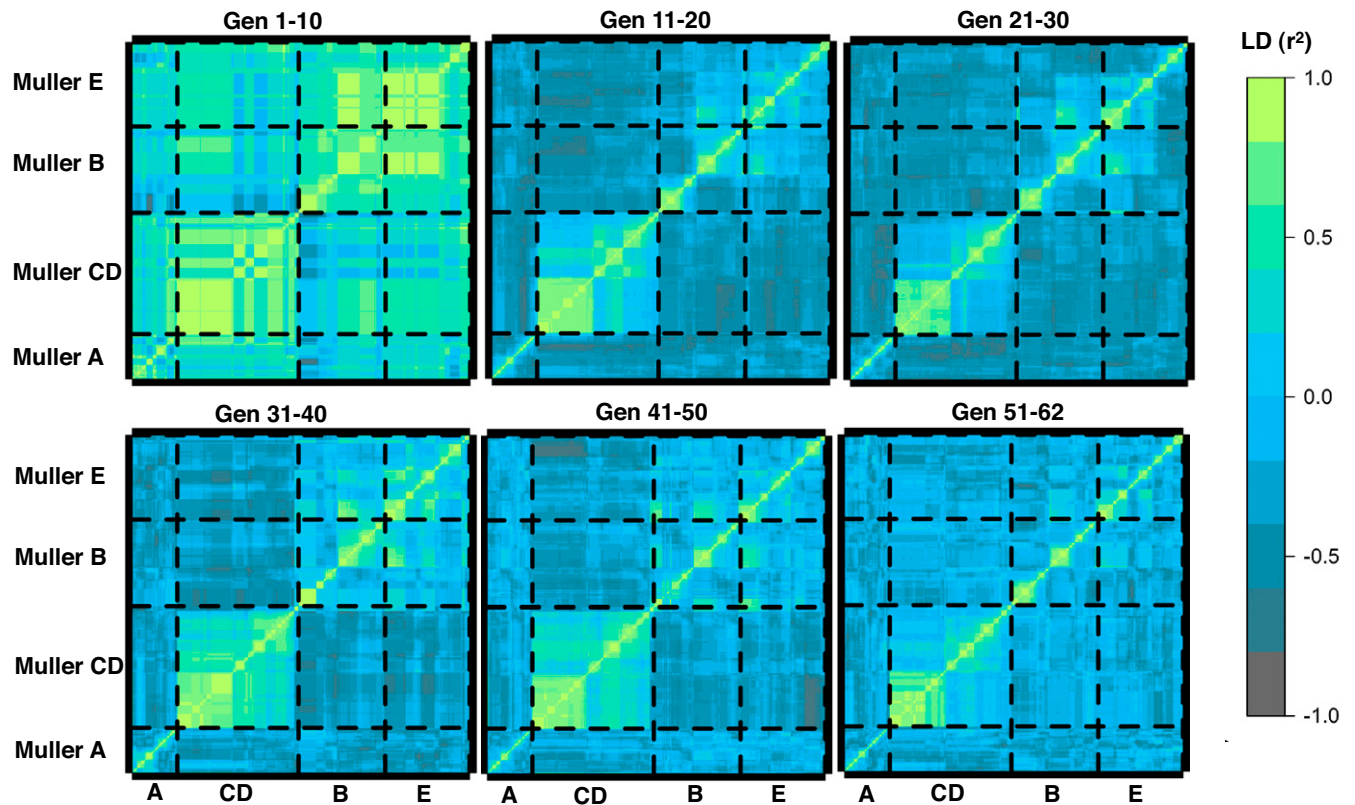
[1c]

Fig. 4. LD (r^2) among K-means clusters across Muller elements. Genome-wide LD decays with admixture. However, LD remains high within Muller CD and some regions in Muller B and E.

As the general conditions for the stability of these three equilibria are complex, we consider equilibrium stability and model dynamics for four specific subparameter cases, cases I, II, III, and IV described below. To explore the parameter space that could result in observed karyotypes in the end of the hybrid swarm experiment, we initialized the dynamics with even ancestry and sex ratio, which is consistent with the initialization of the hybrid swarm experiment.

We focus on the equilibrium in Eq. **1b** where (A_x, A_x) and (A_x, N_y) are the predominant karyotypes because this equilibrium is the most consistent with the observed karyotype frequency at generation 62 of the hybrid swarm experiment. The temporal dynamics of the theoretical model exhibit no cyclic behavior (all eigenvalues are real). Hence, while the karyotypes at generation 62 of the experiment are not yet fixed at this equilibrium, the dynamical trend is constant with an approach to this fixed state. In all four parameter cases, we include

selection favoring the neo-X ($s_x > 0$) and incompatibility between heterospecific chromosomes ($\rho > 0$) as empirically established. The remaining parameters conditions for each of the four cases are described below.

In case I we consider the effect of meiotic drive within *D. nasuta* ($\mu_N \geq 0$) and/or heterospecific meiotic drive ($\mu_H \geq 0$) in the absence of any form of selective disadvantage to A_y ($s_y = 0$, $\mu_A = 0$). The analytical local stability analysis reveals that under no such condition is the focal equilibrium in Eq. **1b** stable. Hence, the observation of the empirical karyotype frequencies requires selection against A_y carrying zygotes ($s_Y \geq 0$) and/or gametic selection against A_y via *D. albomicans*–specific meiotic drive ($\mu_A \geq 0$).

To examine when *D. albomicans* meiotic drive alone can facilitate the fixation of the A_xA_x/A_xN_y karyotype, in case II we allow $\mu_A > 0$ and setting the remaining parameters to 0 ($s_Y = \mu_H = \mu_N = 0$). The global stability of the equilibria

Table 1. Genomic cline parameter estimates of females and males in various generations

Generations	Parameter	Female estimate	Female *P* value	Male estimate	Male *P* value
11–20	Alpha	**0.21**	**0.01**	−0.03	0.55
	Beta	0.26	0.23	0.05	0.82
21–30	Alpha	0.08	0.24	−0.06	0.42
	Beta	0.30	0.12	−0.01	0.97
31–40	Alpha	**0.67**	**<10–5**	**−0.18**	**0.03**
	Beta	−0.24	0.22	−0.34	0.31
41–50	Alpha	0.08	0.60	−0.04	0.66
	Beta	0.24	0.65	0.20	0.55
51–62	Alpha	0.01	0.93	−0.09	0.20
	Beta	0.50	0.13	0.56	0.08

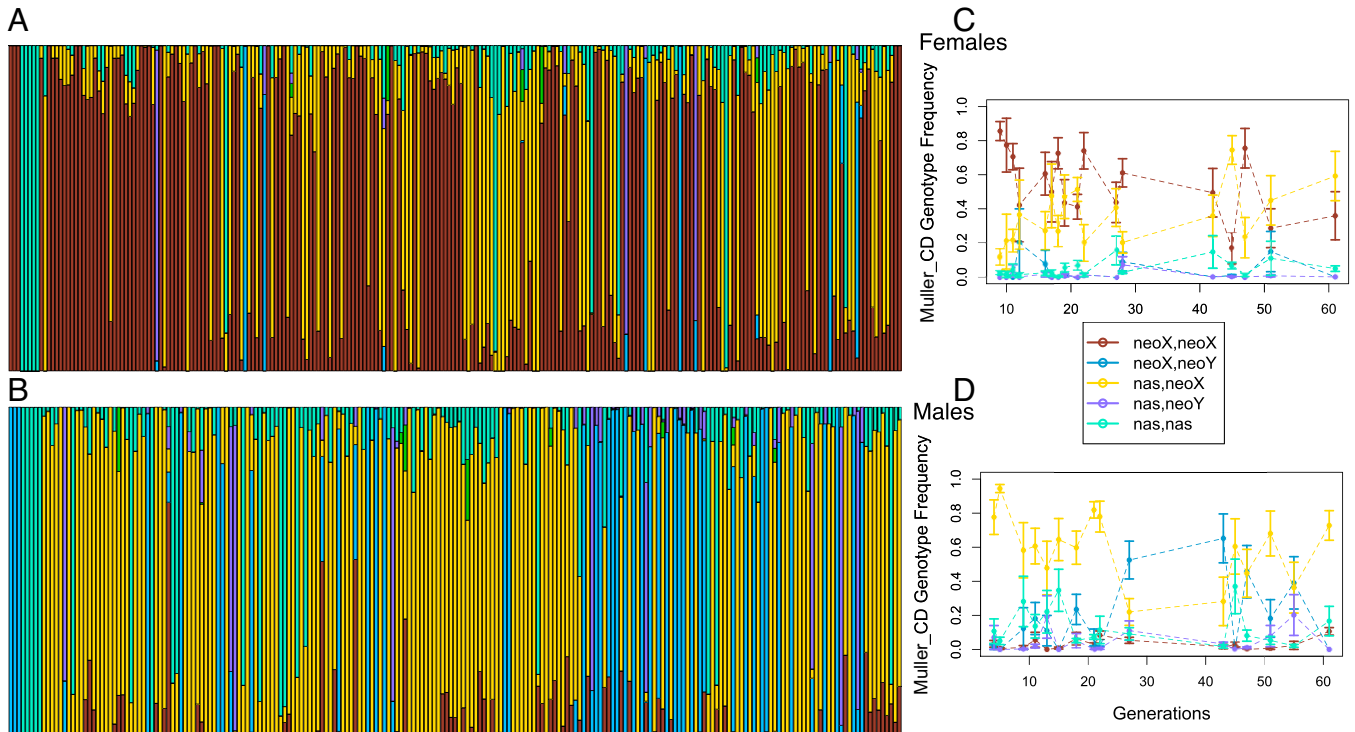Alpha and Beta values that are significantly different from zero are bold.

Fig. 5. Sex stage–dependent introgression asymmetry within Muller CD. The proportion of genotypes within Muller CD for each (*A*) female and (*B*) male hybrid sampled and ordered from generation 0 to 62. The color code for genotypes is as follows: (neo-X, neo-X) in brown, (neo-X, neo-Y) in blue, (neo-X, *D. nasuta* Muller CD) in gold, (neo-Y, *D. nasuta* Muller CD) in purple, and (*D. nasuta* Muller CD, *D. nasuta* Muller CD) in turquoise. (*C*) (neo-X, neo-X) was the predominant genotype in female throughout the generations sampled, but (*D*) the heterozygous genotype (neo-X, *D. nasuta* Muller CD) and (neo-X, neo-Y) alternate in being the predominant male genotype. The error bars represent SEMs.

given the initial conditions of the hybrid swarm experiment is shown in Fig. 6*B*, where the boundary between the equilibria in Eq. **1c** (dotted) and Eq. **1b** (solid yellow) is given by $\rho = \frac{s_x}{1+s_x}$, and the boundary between the equilibria in Eq. **1a** (fixation of $A_x A_x / A_x A_y$), Eq. **1b** (fixation of $A_x A_x / A_x N_y$), and Eq. **1c** (fixation of $N_x N_x / N_x N_y$) is determined numerically. The resulting parameter range over where the focal equilibrium (yellow region) is stable increases with an increasing strength of the *D. albomicans* meiotic drive μ_A.

In contrast, in case III we consider if and when the focal equilibrium is stable given only selection against A_y carrying zygotes $(s_y > 0, \mu_A = \mu_H = \mu_N = 0)$. The resulting global stability analysis is shown in Fig. 6*B*. As with case II, the boundary between the equilibria in Eq. **1a** and Eq. **1b** and Eq. **1c** is determined numerically, and the boundary between Eq. **1b** (yellow) and Eq. **1c** (dotted) is given by $\rho = \frac{s_y}{1+s_y}$. The parameter range under which the focal equilibrium is stable is relatively small, requiring s_y to be large.

Direct application of cases II and III to the empirical system is limited as both assume $\mu_H = 0$, whereas the empirical estimates of $\mu_H = 0.12$ (Fig. 6*A*). While we are not able to examine the case of $\mu_H \neq 0$ in general, in case IV we examine three specific parameter combinations of μ_A and s_y, given $\mu_H = 0.12$. Overall, we find that μ_H hinders the fixation of the $A_x A_x / A_x N_y$ karyotypes (Fig. 6*D*). For this focal equilibrium to be stable across a substantial region of parameter space requires the presence of both strong zygotic selection s_y and gametic selection μ_A against A_y.

Discussion

By tracking *D. albomicans*–*D. nasuta* ancestry in hybrid swarms over many generations, we revealed the multifaceted roles of neo-sex chromosome evolution in introgression across this species boundary: overall, the neo-sex chromosomes serve as sex-dependent asymmetrical introgression barriers between these diverging species. Limited introgression was observed within the overlapping paracentric inversions located on the neo-sex chromosome/Muller-CD. Female-specific *D. albomicans*–biased introgression of the neo-X chromosome is consistent with the relative fitness advantage of neo-X versus the unfused *D. nasuta* type (Fig. 5*C*) and neo-X meiotic drive. Despite the fact that the neo-Y is the more compatible pairing partner of the neo-X relative to the *D. nasuta* unfused type, we did not observe neo-X–facilitated neo-Y introgression. Instead, we observed male-biased heterosis (Fig. 5*D*). Theory suggests such a surprising sex-dependent pattern of introgression relies on *D. albomicans*–specific meiotic drive and neo-Y disadvantage in concert with neo-X advantage and heterospecific chromosome pairing disadvantage. Sex ratio assays revealed interspecific sex chromosome drive (Fig. 6*A*), and previous sequence and expression analysis showed that the neo-Y chromosome shows moderate levels of degeneration and may thus be selected against in hybrid males (19). Our population model suggests that the interplay among meiotic drive, neo-Y degeneration disadvantage, neo-X advantage, and pairing incompatibility can account for the sex-dependent asymmetrical introgression barrier effect of the neo-sex chromosomes.

Introgression Barrier and Speciation. Sex chromosomes are increasingly recognized as barriers of introgression across a diverse group of organisms (6–8, 39, 40). However, the mechanism of such a barrier effect is not well understood. By tracking the behavior of newly formed sex chromosomes at an incomplete species boundary, we dissected barrier effects of sex chromosome evolution on introgression. We observed a strong
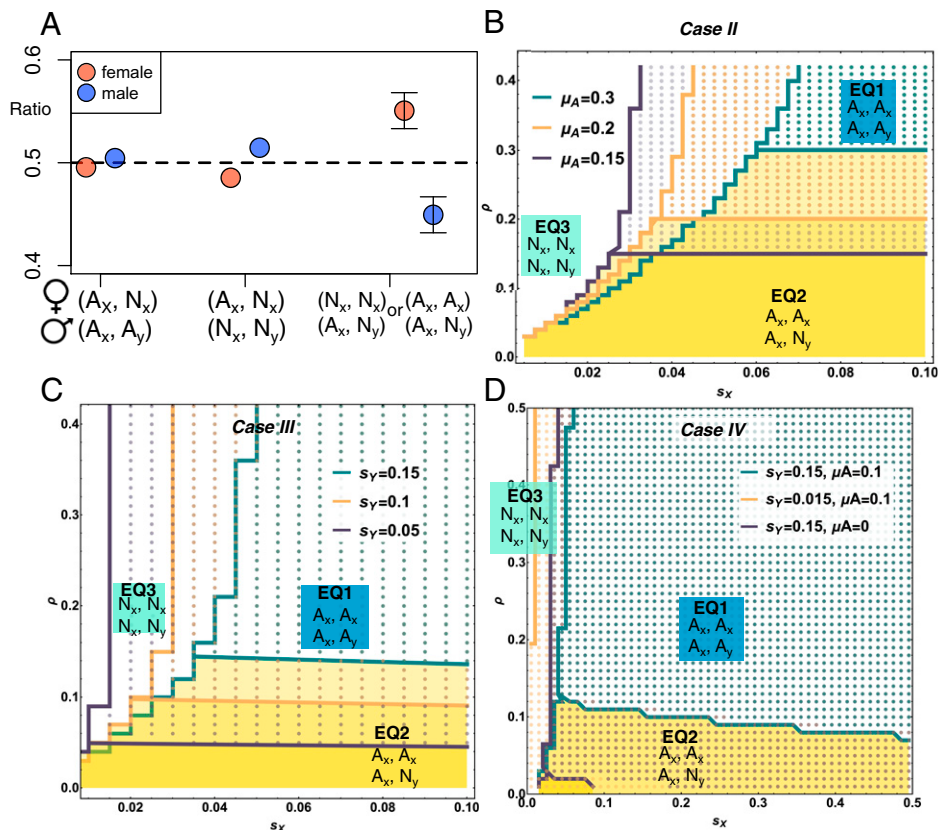
Fig. 6. Parameter space in which the system reaches each of the three stable equilibria based on the initial condition of the hybrid swarm experiment. The parameter spaces in which equilibrium EQ1 (Eq. **1**a, dotted region), EQ2 (Eq. **1**b, yellow), and EQ3 (Eq. **1**c, white) are reached given the initial conditions of the hybrid swarm experiment. (*A*) Sex ratio assay reveals putative meiotic drive rate in conspecific (μ_A, μ_N) and heterospecific (μ_H) conditions. Shown are inferred sex ratios in backcrosses, where female genotypes are listed above male genotypes. Conspecific meiotic drive rates μ_A and μ_N are inferred from (A_x, N_x) × (A_x, A_y) and (A_x, N_x) × (N_x, N_y) crosses, respectively. No significantly sex ratio distortion is observed within *D. albomicans* or *D. nasuta*. However, there was significant sex ratio distortion between species (heterospecific meiotic drive μ_H), which is estimated to be 0.12. (*B*) In the population genetic model we fixed meiotic drive rates based on sex ratio estimates, where $\mu_A = 0$, $\mu_H = 0$, $\mu_N = 0$, $s_Y > 0$. The conditions for the hybrid swarm to reach EQ2, with (A_x, A_y) and (A_x, N_y) genotypes, are delineated in the yellow shades in the space of ρ, s_X, and μ_A. (*C*) For case III, where $\rho > 0$, $s_X > 0$, $s_Y > 0$ and $\mu_A = \mu_N = \mu_H = 0$, to reach EQ2, as observed in the hybrid swarm, requires strong s_Y and low ρ. (*D*) Result for case IV, where $\rho > 0$, $s_X > 0$, $s_Y > 0$ and $\mu_A > 0$, $\mu_N = 0$, $\mu_H = 0.12$. To reach EQ2 in this case requires selection against the neo-Y, moderate selection for the neo-X, and weak hybrid incompatibility.

introgression barrier effect within the recently formed neo-sex chromosome (Fig. 1), which is partly explained by two overlapping inversions on Muller CD (Fig. 2). In addition, pairing incompatibility between the *D. albomicans* fused and *D. nasuta* unfused genotypes can result in increased rates of aneuploidy (23) and may further explain the reduced introgression in Muller CD. After the fusion of the sex chromosome and autosome forming the neo-sex chromosome, the neo-sex chromosomes may accumulate sexual antagonistic loci (41, 42), which can also prevent introgression of heterospecific variants.

However, heterospecific chromosomal incompatibility is insufficient to form a complete reproductive barrier between this species pair. Even within the sex chromosome, there was excessive heterospecific genotype (neo-X and *D. nasuta* Muller CD) in hybrid males and excessive neo-X relative to the genome background in female hybrids, which could deteriorate the species boundaries. We found that neo-X meiotic drive and neo-Y degeneration load could counteract chromosomal incompatibility and facilitate introgression across the species boundary. Together, opposing evolutionary forces acting on the neo-sex chromosomes underlie the conflicting role of neo-sex chromosome evolution in the formation and maintenance of this species boundary.

Sex-Dependent Asymmetrical Introgression. In addition to the barrier effect, we also observed sex-dependent asymmetrical

introgression associated with the neo-sex chromosome (Fig. 3). In females, there was *D. albomicans*–biased introgression, whereas there was heterosis in males (Fig. 5 *C* and *D*). The fused *D. albomicans* neo-X chromosome is thought to be advantageous over the unfused primitive haplotype (23). For the neo-X chromosome to increase to high frequency, it has to overcome meiotic structural incompatibility with its unfused homolog. Female *D. albomicans*–biased neo-X introgression (Fig. 5) supports neo-X advantage since advantageous parental haplotypes tend to dominate hybrid genomes (43). The neo-X chromosome may be preferentially transmitted to the next generation over the unfused Muller CD, by hijacking the asymmetric divisions of female meiosis (female meiotic drive) (41). We used sequencing of a large pool of backcross progeny embryos to test for deviations from Mendelian segregation (following ref. 42) but found no evidence of meiotic drive in female F1 hybrids (*SI Appendix*, Fig. S8). This suggests that the selective advantage of the neo-X is not due to some conflict during female meiosis.

However, neo-X advantages and/or pairing incompatibility does not explain heterosis in males (Fig. 5*D*). Surprisingly, the heterozygous (neo-X, *D. nasuta* Muller CD) genotype occurred more frequently than the neo-X and neo-Y combination in most time points of the hybrid swarm experiment (Fig. 5 and *SI Appendix*, Fig. S7). Notably, the heterosis in the heterogametic sex is opposite to Haldane's rule.

Population genetic modeling suggests that the interplay among neo-Y disadvantage and meiotic drive in *D. albomicans*, combined with neo-X advantage and heterospecific pairing incompatibility, can explain the observed male heterosis and female *D. albomicans*–biased introgression in Muller CD (Figs. 5 and 6). With moderate meiotic drive and selective disadvantage of neo-Y, at moderate pairing incompatibility and selective advantage of neo-X, the system could reach the (neo-X, *D. nasuta* Muller CD) equilibrium in males. Meiotic drive alleles have been characterized in *D. albomicans* Muller CD with quantitative trait locus mapping (27), in addition to neo-X advantage (23), and chromosomal pairing incompatibility between *D. nasuta* Muller CD and the fused type (23, 25). However, in the parental strains involved in the hybrid swarm experiment, we did not observe intraspecific meiotic drive in *D. albomicans* or *D. nasuta*, but there was low to moderate level of heterospecific meiotic drive (∼12%, female bias). Patterns of molecular evolution and gene expression on the neo-Y of 15112-1751.03, the *D. albomicans* parental strain we used, revealed moderate levels of degeneration, with dozens of neo-Y–linked genes showing stop codons and frameshift mutations and reduced gene expression (21). This supports selection against the neo-Y in hybrid males (s_Y). Our population model (Fig. 6*D*) suggests that under the initial condition of the experiment and estimations of meiotic drive rates, selection against the neo-Y ($s_Y > 0$) is required to observe excessive (neo-X, *D. nasuta Muller CD*) combination, the male-specific Muller CD heterosis.

Alternative Oscillation of (neo-X, *D. nasuta* Muller CD) and (neo-X, neo-Y). The most abundant Muller CD genotypes in males were (neo-X, *D. nasuta* Muller CD). However, an exception occurred between generations 30 and 40, when (neo-X, neo-Y) became more abundant (Fig. 5*D* and *SI Appendix,* Fig. S7); such oscillation suggests that the system might not have reached equilibrium. The low frequency of (*D. nasuta* X, *D. nasuta* Muller CD) throughout the experiment suggests that neo-X advantage could be strong. When neo-X increases in frequency in females, in males, (neo-X, *D. nasuta* Muller CD) became more prevalent, instead of (neo-X, neo-Y). The neo-Y haplotypic frequency in males is less associated with neo-X frequency in females than *D. nasuta* unfused haplotype, which is likely due to the opposite directions of selection in neo-X versus neo-Y. Toward the last generation, males were mostly (neo-X, *D. nasuta* Muller CD), while other genotypes were almost lost.

This is similar to the EQ2 condition, at which the system is more likely to arrive when there is selective advantage of neo-X, selective disadvantage of neo-Y, *D. albomicans* meiotic drive, and pairing incompatibility (Fig. 6).

Neo-Sex Chromosome Evolution and Speciation. Neo-sex chromosomes may play an important role in speciation in a wide variety of species. The origin of a neo-sex chromosome could immediately incur genetic incompatibility and contribute to reproductive isolation (24, 44). In addition, neo-sex chromosomes may accumulate sexually antagonistic variants, and sexual antagonistic coevolution can speed up divergent evolution and speciation (12, 45). Unresolved genetic conflict at sex chromosomes could also facilitate introgression, allowing genetic counterparts to escape from the conspecific arms race (46). We found evidence for conflicting roles of neo-sex chromosome evolution in the maintenance of genomic barriers of reproductive isolation. On one hand, we observed suppressed ancestry turnovers within the neo-sex chromosomes relative to the rest of the genome, which facilitates speciation. On the other hand, we observed sex-dependent asymmetrical introgression within the neo-sex chromosome that appears to be mediated by a complex interplay of neo-X advantage, meiotic drive, neo-Y degeneration, and pairing incompatibility. While our observations are based on an artificial hybrid swarm of a particular species pair of *Drosophila* under a controlled laboratory environment, our experiment provides a framework of how neo-sex chromosome evolution and speciation can contribute to organismal diversity in the wild. We characterized multiple conflicting evolutionary forces that could be parsed out in natural hybrid populations across the tree of life for understanding the diverse roles of neo-sex chromosome evolution in speciation.

Conclusion. Here we characterized and dissected sex-dependent asymmetrical barriers to introgression in the early stage of divergence that are affected by the evolution of neo-sex chromosomes. Such complex genomic barrier effect can be explained by the interplay of neo-X advantage and neo-Y degenerative disadvantage, chromosomal pairing incompatibility, and meiotic drive within the neo-sex chromosome.

1. C. Darwin, *On the Origin of the Species* (John Murray, 1859).
2. B. A. Payseur, L. H. Rieseberg, A genomic perspective on hybridization and speciation. *Mol. Ecol.* **25**, 2337–2360 (2016).
3. P. Nosil, J. L. Feder, Genomic divergence during speciation: Causes and consequences. *Philos. Trans. R. Soc. Lond. B Biol. Sci.* **367**, 332–342 (2012).
4. C. R. Campbell, J. W. Poelstra, A. D. Yoder, What is speciation genomics? The roles of ecology, gene flow, and genomic architecture in the formation of species. *Biol. J. Linn. Soc. Lond.* **124**, 561–583 (2018).
5. O. Seehausen *et al.*, Genomics and the origin of species. *Nat. Rev. Genet.* **15**, 176–192 (2014).
6. D. C. Presgraves, Evaluating genomic signatures of "the large X-effect" during complex speciation. *Mol. Ecol.* **27**, 3822–3830 (2018).
7. J. P. Masly, D. C. Presgraves, High-resolution genome-wide dissection of the two rules of speciation in Drosophila. *PLoS Biol.* **5**, e243 (2007).
8. M. J. O'Neill, R. J. O'Neill, Sex chromosome repeats tip the balance towards speciation. *Mol. Ecol.* **27**, 3783–3798 (2018).
9. A. Qvarnström, R. I. Bailey, Speciation through evolution of sex-linked genes. *Heredity* **102**, 4–15 (2009).
10. J. A. Coyne, Genetics and speciation. *Nature* **355**, 511–515 (1992).
11. M. Kirkpatrick, N. Barton, Chromosome inversions, local adaptation and speciation. *Genetics* **173**, 419–434 (2006).
12. J. Kitano *et al.*, A role for a neo-sex chromosome in stickleback speciation. *Nature* **461**, 1079–1083 (2009).
13. R. R. Bracewell, B. J. Bentz, B. T. Sullivan, J. M. Good, Rapid neo-sex chromosome evolution and incipient speciation in a major forest pest. *Nat. Commun.* **8**, 1593 (2017).
14. D. Bachtrog, The speciation history of the *Drosophila nasuta* complex. *Genet. Res.* **88**, 13–26 (2006).
15. H.-Y. Chang, F. J. Ayala, On the origin of incipient reproductive isolation: The case of *Drosophila albomicans* and *D. nasuta*. *Evolution* **43**, 1610–1624 (1989).
16. Y.-K. Kim, D. R. Phillips, Y. Tao, Nearly random mating occurs between *Drosophila nasuta* and *D. albomicans*. *Ecol. Evol.* **3**, 2061–2074 (2013).
17. H.-Y. Chang, F. J. Ayala, On the origin of incipient reproductive isolation: The case of *Drosophila albomicans* and *D. nasuta*. *Evolution (N. Y.)* **43**, 1610–1624 (1989).
18. Y. Inoue, O. Kitagawa, Incipient reproductive isolation between *Drosophila nasuta* and *Drosophila albomicans*. *Genet. Sel. Evol.* **22**, 31–46 (1990).
19. K. I. Wakahama *et al.*, Genetic studies of the *Drosophila nasuta* subgroup, with notes on distribution and morphology. *Jpn. J. Genet.* **57**, 113–141 (1982).
20. K. H. C. Wei, D. Bachtrog, Ancestral male recombination in *Drosophila albomicans* produced geographically restricted neo-Y chromosome haplotypes varying in age and onset of decay. *PLoS Genet.* **15**, e1008502 (2019).
21. T. Ohsako, T. Aotsuka, O. Kitagawa, The origins of the Japanese mainland population of *Drosophila albomicans*. *Jpn. J. Genet.* **69**, 183–194 (1994).
22. Y. C. Yu, F. J. Lin, H. Y. Chang, Stepwise chromosome evolution in *Drosophila albomicans*. *Heredity* **83**, 39–45 (1999).
23. L. Z. Carabajal Paladino *et al.*, Sex chromosome turnover in moths of the diverse superfamily gelechioidea. *Genome Biol. Evol.* **11**, 1307–1319 (2019).
24. Y.-C. Yu, F.-J. Lin, H. Chang, Karyotype polymorphism in hybrid populations of *Drosophila nasuta* and *D. albomicans*. *Zool. Stud.* **26**, 251–259 (1997).
25. Y. Yung-Yu, L. Fei-Jann, H. Chang, Sex ratio distortion in hybrids of *Drosophila albomicans* and *D. nasuta*. *Zool. Stud.* **43**, 622–628 (2004).
26. L. Zhang, T. Sun, F. Woldesellassie, H. Xiao, Y. Tao, Sex ratio meiotic drive as a plausible evolutionary mechanism for hybrid male sterility. *PLoS Genet.* **11**, e1005073 (2015).

27. D. Mai, D. Bachtrog, Molecular characterization of inversion breakpoints in the *Drosophila nasuta* species group. bioRxiv [Preprint] (2021). https://doi.org/10.1101/2021.06.01.446624 (Accessed 6 January 2020).

28. M. Baym *et al.*, Inexpensive multiplexed library preparation for megabase-sized genomes. *PLoS One* **10**, e0128036 (2015).

29. A. M. Bolger, M. Lohse, B. Usadel, Trimmomatic: A flexible trimmer for Illumina Sequence Data. *Bioinformatics*, btu170 (2014). http://www.usadellab.org/cms/?page=trimmomatic (Accessed 18 April 2022).

30. D. Mai, M. J. Nalley, D. Bachtrog, Patterns of genomic differentiation in the *Drosophila nasuta* species complex. *Mol. Biol. Evol.* **37**, 208–220 (2020).

31. K. M. Wong Miller, R. R. Bracewell, M. B. E. Eisen, D. Bachtrog, Patterns of genome-wide diversity and population structure in the *Drosophila athabasca* species complex. *Mol. Biol. Evol.* **34**, 1912–1923 (2017).

32. H. Li, Aligning new-sequencing reads by BWA (2010). https://www.broadinstitute.org/files/shared/mpg/nextgen2010/nextgen_li.pdf. Accessed 3 January 2020.

33. P. Danecek *et al.*; 1000 Genomes Project Analysis Group, The variant call format and VCFtools. *Bioinformatics* **27**, 2156–2158 (2011).

34. R. Corbett-Detig, R. Nielsen, A hidden Markov model approach for simultaneously estimating local ancestry and admixture time using next generation sequence data in samples of arbitrary ploidy. *PLoS Genet.* **13**, e1006529 (2017).

35. E. Forgy, Cluster analysis of multivariate data: Efficiency versus interpretability of classifications. *Biometrics* **21**, 768–769 (1965).

36. B. M. Fitzpatrick, Estimating ancestry and heterozygosity of hybrids using molecular markers. *BMC Evol. Biol.* **12**, 131 (2012).

37. Z. Gompert, C. A. Buerkle, Bayesian estimation of genomic clines. *Mol. Ecol.* **20**, 2111–2127 (2011).

38. J. von Neumann, R. H. Kent, H. R. Bellinson, B. I. Hart, The mean square successive difference. *Ann. Math. Stat.* **12**, 153–162 (1941).

39. D. E. Irwin, Sex chromosomes and speciation in birds and other ZW systems. *Mol. Ecol.* **27**, 3831–3851 (2018).

40. B. Charlesworth, J. A. Coyne, N. H. Barton, The relative rates of evolution of sex chromosomes and autosomes. *Am. Nat.* **130**, 113–146 (1987).

41. D. Charlesworth, Evolution of recombination rates between sex chromosomes. *Philos. Trans. R. Soc. Lond. B Biol. Sci.* **372**, 20160456 (2017).

42. D. Bachtrog, The temporal dynamics of processes underlying Y chromosome degeneration. *Genetics* **179**, 1513–1525 (2008).

43. D. R. Matute *et al.*, Rapid and predictable evolution of admixed populations between two Drosophila species pairs. *Genetics* **214**, 211–230 (2020).

44. G. Dixon, J. Kitano, M. Kirkpatrick, The origin of a new sex chromosome by introgression between two stickleback fishes. *Mol. Biol. Evol.* **36**, 28–38 (2019).

45. C. A. Muirhead, D. C. Presgraves, Satellite DNA-mediated diversification of a sex-ratio meiotic drive gene family in *Drosophila*. *Nat. Ecol. Evol.* **5**, 1604–1612 (2021).

46. C. D. Meiklejohn *et al.*, Gene flow mediates the role of sex chromosome meiotic drive during complex speciation. *eLife* **7**, e35468 (2018).